

Geometry of the generalized Bloch sphere for qutrit

Sandeep K. Goyal,^{1,*} B. Neethi Simon,^{2,†} Rajeev Singh,^{1,‡} and Sudhavathani Simon^{3,§}

¹*Optics & Quantum Information Group, The Institute of Mathematical Sciences, Tharamani, Chennai 600 113*

²*Department of Mechanical Engineering, SSN College of Engineering, SSN Nagar, OMR, Chennai 603 110*

³*Department of Computer Science, Women's Christian College, Chennai 600 006, India*

The geometry of the generalized Bloch sphere Ω_3 , the state space of a qutrit is studied. Closed form expressions for Ω_3 , its boundary $\partial\Omega_3$, and the set of extremals Ω_3^{ext} are obtained by use of an elementary observation. These expressions and analytic methods are used to classify the 28 two-sections and the 56 three-sections of Ω_3 into unitary equivalence classes, completing the works of earlier authors. It is shown, in particular, that there are families of two-sections and of three-sections which are equivalent geometrically but not unitarily, a feature that does not appear to have been appreciated earlier. A family of three-sections of obese-tetrahedral shape whose symmetry corresponds to the 24-element tetrahedral point group T_d is examined in detail. This symmetry is traced to the reduction of the adjoint representation of $SU(3)$, the symmetry underlying Ω_3 , into direct sum of the two-dimensional and the two (inequivalent) three-dimensional irreducible representations of T_d .

PACS numbers: 03.65.-w, 03.65.Ta, 03.65.Fd, 03.63.Vf

I. INTRODUCTION

States of a d -level quantum system are in one-to-one correspondence with positive semidefinite unit-trace operators in a d -dimensional Hilbert space \mathcal{H} . The defining properties of these density operators or density matrices ρ are: (i) $\rho^\dagger = \rho$, (ii) $\rho \geq 0$, and (iii) $\text{tr} \rho = 1$. The collection of all possible density operators of a d -level system is its state space Ω_d . Pure states correspond to the further matrix condition $\rho^2 = \rho$ which is equivalent to the scalar condition $\text{tr} \rho^2 = 1$. All other states are mixed states. It follows from definition that *the quantum state space is a convex set*. That is, convex combination of density operators always results in density operator: $\rho_j \in \Omega_d$, $j = 0, 1, \dots, \ell$ implies $\sum_j p_j \rho_j \in \Omega_d$ for every set $\{p_j\}$ with $p_j > 0$, $\sum_j p_j = 1$.

The importance of a good understanding of the geometry of Ω_d is evident. The structure of Ω_2 , the state space of a two-level system or qubit is simple: it is the Bloch (or Poincaré) sphere. But the structure of Ω_d , the *generalized Bloch sphere*, is much richer for $d \geq 3$, and has attracted the attention of many authors [1–33].

In order to get a quick partial insight into this richness several authors have looked at sections of Ω_d . The original motivation for considering such sections comes from Bloore [1] who examined the five-section of Ω_3 corresponding to density matrices whose entries are all *real*, and noted that this five-section has a three-section of the shape of a tetrapack. [As we shall see below, there exist also other three-sections of Ω_3 of precisely this shape.] Two-sections have been considered

by Kimura [6], Kimura and Kossakowski [7], Mendas [8], Jakobczyk and Siennicki [9], and Kryszewski and Zachcial [10]. The work of Mendas [8] aims also at a classification of the 56 three-sections of Ω_3 using Monte Carlo sampling.

We present in this paper an analysis of the structure of Ω_3 using analytic methods. For purpose of comparison we begin in Section 2 with a brief consideration of Ω_2 . In Section 3 we use the elementary observation that there exists within the ‘unit sphere’ S^7 in \mathbb{R}^8 no singular (hermitian) matrix which is indefinite to derive *closed-form expressions* for Ω_3 , its boundary $\partial\Omega_3$, and for the set of extremals Ω_3^{ext} . We use these closed-form expressions to classify in Section 4 the 28 two-sections of Ω_3 into five unitary equivalence classes of four geometrically different shapes. The 56 three-sections are shown in Section 5 to group themselves into ten unitary inequivalence classes of only seven geometrically different shapes, and the results are contrasted with those of Mendas [8].

One family of three-sections has an interesting geometric shape, obese-tetrahedron, having symmetry that corresponds to the 24-element tetrahedral group T_d familiar from the context of point groups. We study this family in considerable detail in Section 6, and trace this T_d symmetry consisting of ‘proper and improper’ rotations to a discrete subgroup of proper rotations in $SO(3) \subset SU(3)$. This is the subgroup for which the eight-dimensional adjoint representation of $SU(3)$ reduces to direct sum of one two-dimensional and two (inequivalent) three-dimensional irreducible representations of T_d . We conclude in Section 7 with some final remarks.

II. TWO-LEVEL SYSTEMS: BLOCH SPHERE

The density operator in this case is a hermitian, positive (semidefinite) 2×2 matrix of unit trace. The unit

*Electronic address: goyal@imsc.res.in

†Electronic address: neethisimon@gmail.com

‡Electronic address: rajeev@imsc.res.in

§Electronic address: sudhasimon@gmail.com

matrix $\sigma_0 \equiv \mathbb{I}_{2 \times 2}$ along with the Pauli matrices satisfy

$$\begin{aligned} \sigma_j \sigma_k + \sigma_k \sigma_j &= 2\sigma_0 \delta_{jk}, \quad \sigma_j \sigma_k - \sigma_k \sigma_j = 2i\epsilon_{jkl} \sigma_\ell, \\ \text{tr } \sigma_\mu \sigma_\nu &= 2\delta_{\mu\nu}, \quad \mu, \nu = 0, 1, 2, 3; \quad j, k, \ell = 1, 2, 3. \end{aligned}$$

They form a complete set of hermitian orthogonal matrices, and since any 2×2 hermitian matrix can be expressed as a unique linear combination of these matrices, with *real* coefficients, we have

$$\rho = \rho(\mathbf{n}) = \frac{1}{2}(\sigma_0 + \mathbf{n} \cdot \boldsymbol{\sigma}), \quad \mathbf{n} \in \mathbb{R}^3. \quad (1)$$

That the coefficient of σ_0 is $1/2$ follows from and ensures $\text{tr } \rho = 1$. Positivity of this hermitian unit trace expression demands $|\mathbf{n}|^2 = \mathbf{n} \cdot \mathbf{n} \leq 1$. Indeed, the eigenvalues of $\rho(\mathbf{n})$ are seen to be $(1 \pm |\mathbf{n}|)/2$.

It follows that the states are in one-to-one correspondence with the points on or inside the closed unit ball in \mathbb{R}^3 , centered at the origin of \mathbb{R}^3 . This is the Bloch or Poincaré ball. Points on the boundary S^2 correspond to pure states: the unit vector $|\psi\rangle = e^{i\alpha} \begin{pmatrix} \cos \theta/2 \\ e^{i\phi} \sin \theta/2 \end{pmatrix}$ which corresponds to the one-dimensional projector

$$\rho(\theta, \phi) = \frac{1}{2} \begin{pmatrix} 1 + \cos \theta & \sin \theta e^{-i\phi} \\ \sin \theta e^{i\phi} & 1 - \cos \theta \end{pmatrix}, \quad (2)$$

is seen to be represented by unit vector $\mathbf{n}(\theta, \phi) = (\sin \theta \cos \phi, \sin \theta \sin \phi, \cos \theta) \in S^2$. It is clear that orthogonal pure states occupy antipodal points on S^2 . The interior points of the unit ball correspond to mixed states. In particular the centre $\mathbf{n} = 0$ corresponds to the maximally mixed state $\rho = \frac{1}{2}\sigma_0$.

The special property of this convex set or state space Ω_2 which is not shared by n -level systems with $n > 2$ is this: every boundary point is an extremal. There exists another, related aspect in which the quantum two-level system differs from n -level systems with $n \geq 3$. Unitary evolutions $\rho \rightarrow \rho' = U\rho U^\dagger$, $U \in SU(2)$ act on $\Omega_2 \subset \mathbb{R}^3$ through $SO(3)$ rotations arising from the adjoint representation of $SU(2)$. And S^2 , the boundary of Ω_2 is a *single orbit* under this action. This does not hold for Ω_d , $d \geq 3$. While it is true that unitary evolutions $\rho \rightarrow \rho' = U\rho U^\dagger$, $U \in SU(d)$ continue to act as rotations on $\Omega_d \subset \mathbb{R}^{d^2-1}$ through the adjoint representation, the $SU(d)$ orbit of pure states which necessarily corresponds to the $2(d-1)$ -dimensional manifold $SU(d)/SU(d-1) = CP^{d-1}$ is a measure zero subset of the (d^2-2) -dimensional boundary $\partial\Omega_d$: the boundary of Ω_d consists of a *continuum of distinct* $SU(d)$ orbits.

III. BLOCH REPRESENTATION FOR THE QUTRIT

In place of the three Pauli matrices we now need the following eight Gell-Mann λ -matrices to describe a generalization of the Bloch ball representation of qubit to

the case of *three-level system* or *qutrit*:

$$\begin{aligned} \lambda_1 &= \begin{pmatrix} 0 & 1 & 0 \\ 1 & 0 & 0 \\ 0 & 0 & 0 \end{pmatrix}, & \lambda_2 &= \begin{pmatrix} 0 & -i & 0 \\ i & 0 & 0 \\ 0 & 0 & 0 \end{pmatrix}, \\ \lambda_3 &= \begin{pmatrix} 1 & 0 & 0 \\ 0 & -1 & 0 \\ 0 & 0 & 0 \end{pmatrix}, & \lambda_4 &= \begin{pmatrix} 0 & 0 & 1 \\ 0 & 0 & 0 \\ 1 & 0 & 0 \end{pmatrix}, \\ \lambda_5 &= \begin{pmatrix} 0 & 0 & -i \\ 0 & 0 & 0 \\ i & 0 & 0 \end{pmatrix}, & \lambda_6 &= \begin{pmatrix} 0 & 0 & 0 \\ 0 & 0 & 1 \\ 0 & 1 & 0 \end{pmatrix}, \\ \lambda_7 &= \begin{pmatrix} 0 & 0 & 0 \\ 0 & 0 & -i \\ 0 & i & 0 \end{pmatrix}, & \lambda_8 &= \frac{1}{\sqrt{3}} \begin{pmatrix} 1 & 0 & 0 \\ 0 & 1 & 0 \\ 0 & 0 & -2 \end{pmatrix}. \end{aligned}$$

These matrices are familiar as generators of the unimodular unitary group $SU(3)$ in its defining representation. Just like the Pauli matrices these form a *complete* set of hermitian, traceless, trace-orthogonal matrices:

$$\text{tr } \lambda_k \lambda_l = 2\delta_{kl}, \quad k, l = 1, 2, \dots, 8. \quad (3)$$

The algebraic structure of these matrices is determined by the product property [34–37]

$$\lambda_j \lambda_k = \frac{2}{3} \delta_{jk} + d_{jkl} \lambda_l + i f_{jkl} \lambda_l. \quad (4)$$

Separating this product into hermitian and antihermitian parts, we have

$$\begin{aligned} \lambda_j \lambda_k - \lambda_k \lambda_j &= 2i f_{jkl} \lambda_l, \\ \lambda_j \lambda_k + \lambda_k \lambda_j &= \frac{4}{3} \delta_{jk} + 2d_{jkl} \lambda_l. \end{aligned} \quad (5)$$

The expansion coefficients f_{jkl} , the structure constants of the Lie algebra of $SU(3)$, are *totally antisymmetric* in their indices, whereas d_{jkl} are *totally symmetric*. It is useful to list the numerical values of all the independent nonvanishing components of f_{jkl} , d_{jkl} [34–37]:

$$\begin{aligned} f_{123} &= 1, \quad f_{458} = f_{678} = \frac{\sqrt{3}}{2}, \\ f_{147} = f_{246} = f_{257} = f_{345} = f_{516} = f_{637} &= \frac{1}{2}; \\ d_{118} = d_{228} = d_{338} = -d_{888} &= \frac{1}{\sqrt{3}}, \\ d_{146} = d_{157} = -d_{247} = d_{256} &= \frac{1}{2}, \\ d_{344} = d_{355} = -d_{366} = -d_{377} &= \frac{1}{2}, \\ d_{448} = d_{558} = d_{668} = d_{778} &= -\frac{1}{2\sqrt{3}}. \end{aligned} \quad (6)$$

These λ -matrices can be used to describe any 3×3 density matrix ρ in terms of a corresponding 8-dimensional *real* vector \mathbf{n} :

$$\rho(\mathbf{n}) = \frac{1}{3} (\mathbb{I} + \sqrt{3} \mathbf{n} \cdot \boldsymbol{\lambda}), \quad \mathbf{n} \in \mathbb{R}^8. \quad (7)$$

Hermiticity of $\rho(\mathbf{n})$ is ensured by that of the λ -matrices and reality of \mathbf{n} , and unit trace property is ensured by the prefactor $\frac{1}{3}$. Thus, it remains only to choose (restrict) $\mathbf{n} \in \mathbb{R}^8$ such that the matrix $\mathbb{I} + \sqrt{3}\mathbf{n} \cdot \boldsymbol{\lambda}$ is positive semidefinite.

Let Ω_3 be the set of all points $\mathbf{n} \in \mathbb{R}^8$ such that $\mathbb{I} + \sqrt{3}\mathbf{n} \cdot \boldsymbol{\lambda} \geq 0$. Then, by definition, $\Omega_3 \subset \mathbb{R}^8$ is our state space or *generalized Bloch sphere*. We know that Ω_3 is a closed convex set. Our aim here is to develop an understanding of the structure of Ω_3 , and we begin by giving *closed form expressions* for both its boundary $\partial\Omega_3$ and the set of all extremals Ω_3^{ext} , leading eventually to a closed form expression for the convex Ω_3 itself.

A. Extremal points of Ω_3

We begin our analysis by defining a *star-product* $\mathbb{R}^8 \rightarrow \mathbb{R}^8$ on vectors $\mathbf{n} \in \mathbb{R}^8$ through [34–37]

$$(\mathbf{n} * \mathbf{n})_l = \sqrt{3}d_{jkl}n_jn_k. \quad (8)$$

As an immediate consequence and application we have the following expression for the square of any traceless hermitian matrix $\mathbf{n} \cdot \boldsymbol{\lambda}$:

$$\mathbf{n} \cdot \boldsymbol{\lambda} \mathbf{n} \cdot \boldsymbol{\lambda} = \frac{2}{3}\mathbf{n} \cdot \mathbf{n} + \frac{1}{\sqrt{3}}\mathbf{n} * \mathbf{n} \cdot \boldsymbol{\lambda}. \quad (9)$$

Now the necessary and sufficient condition for a density operator $\rho(\mathbf{n})$ to correspond to a pure state, and hence to an extremal of Ω_3 , is that it be a one dimensional projector, i.e., $\rho(\mathbf{n})^2 = \rho(\mathbf{n})$. So we compute

$$\rho(\mathbf{n})^2 = \frac{1}{9} \left(\mathbb{I} + 2\mathbf{n} \cdot \boldsymbol{\lambda} + 2\sqrt{3}\mathbf{n} \cdot \boldsymbol{\lambda} + \sqrt{3}\mathbf{n} * \mathbf{n} \cdot \boldsymbol{\lambda} \right). \quad (10)$$

Equating this expression to $\rho(\mathbf{n}) = (\mathbb{I} + \sqrt{3}\mathbf{n} \cdot \boldsymbol{\lambda})/3$, Eq. (7), we obtain a pair of constraints

$$\mathbf{n} \cdot \mathbf{n} = 1, \quad \mathbf{n} * \mathbf{n} = \mathbf{n} \quad (11)$$

as the defining conditions on points $\mathbf{n} \in \mathbb{R}^8$ in order that $\rho(\mathbf{n}) \in \Omega_3^{\text{ext}} \subset S^7$, the set of all the extremals of our state space Ω_3 . Since we know that these extremals constitute also CP^2 , the manifold of pure states of a three-level quantum system, we may write:

$$\Omega_3^{\text{ext}} = CP^2 = \{ \mathbf{n} \in \mathbb{R}^8 \mid \mathbf{n} \cdot \mathbf{n} = 1, \mathbf{n} * \mathbf{n} = \mathbf{n} \}. \quad (12)$$

Having thus described in *closed form* the four-parameter family of extremals of Ω_3 , we now move on to develop an expression for the boundary $\partial\Omega_3$.

B. Closed-form expressions for the Bloch sphere Ω_3 and its boundary $\partial\Omega_3$

It is clear that the boundary of Ω_3 comprises density matrices which are singular. Thus the boundary points

$\mathbf{n} \in \mathbb{R}^8$ should necessarily satisfy the condition

$$\det \rho(\mathbf{n}) = 0 = \det(\mathbb{I} + \sqrt{3}\mathbf{n} \cdot \boldsymbol{\lambda}),$$

$$\mathbf{n} \cdot \boldsymbol{\lambda} = \begin{pmatrix} n_3 + \frac{1}{\sqrt{3}}n_8 & n_1 - in_2 & n_4 - in_5 \\ n_1 + in_2 & -n_3 + \frac{1}{\sqrt{3}}n_8 & n_6 - in_7 \\ n_4 + in_5 & n_6 + in_7 & -\frac{2}{\sqrt{3}}n_8 \end{pmatrix}. \quad (13)$$

Writing out this requirement in detail, we have

$$3(n_1^2 + n_2^2 + n_3^2 + n_4^2 + n_5^2 + n_6^2 + n_7^2 + n_8^2) - 6n_8 \left(n_1^2 + n_2^2 + n_3^2 - \frac{n_4^2 + n_5^2 + n_6^2 + n_7^2}{2} - \frac{n_8^2}{3} \right) - 6\sqrt{3}(n_1n_4n_6 + n_1n_5n_7 + n_2n_5n_6 - n_2n_4n_7) - 3\sqrt{3}n_3(n_4^2 + n_5^2 - n_6^2 - n_7^2) = 1. \quad (14)$$

Every boundary point $\mathbf{n} \in \partial\Omega_3$ should necessarily satisfy this *cubic* constraint. It is readily verified that $\mathbb{I} + \sqrt{3}\mathbf{n} \cdot \boldsymbol{\lambda}$ is *necessarily indefinite* if $\mathbf{n} \cdot \mathbf{n} > 1$, and therefore nonnegativity of ρ demands that \mathbf{n} should satisfy the additional inequality

$$|\mathbf{n}|^2 \equiv \sum_{j=1}^8 n_j^2 \leq 1. \quad (15)$$

As the final step, we will make use of the following elementary observation.

Theorem: No *singular matrix* of the form $\mathbb{I} + \sqrt{3}\mathbf{n} \cdot \boldsymbol{\lambda}$, with $|\mathbf{n}| \leq 1$, can be indefinite.

Proof: Singularity of $\mathbb{I} + \sqrt{3}\mathbf{n} \cdot \boldsymbol{\lambda}$ implies that the matrix $\mathbf{n} \cdot \boldsymbol{\lambda}$ should necessarily have $-\frac{1}{\sqrt{3}}$ as one of its eigenvalues. Tracelessness of $\mathbf{n} \cdot \boldsymbol{\lambda}$ then implies that the other two eigenvalues be of the form $\mu, \frac{1}{\sqrt{3}} - \mu$. But the condition $|\mathbf{n}| \leq 1$ is equivalent to the requirement that the sum of squares of the eigenvalues of $\mathbf{n} \cdot \boldsymbol{\lambda}$ be bounded by 2 as may be seen from Eq. (9), i.e., $\left(\frac{1}{\sqrt{3}}\right)^2 + \mu^2 + \left(\frac{1}{\sqrt{3}} - \mu\right)^2 \leq 2$. The last inequality obviously forces μ to the range

$$-\frac{1}{\sqrt{3}} \leq \mu \leq \frac{2}{\sqrt{3}}, \quad (16)$$

proving our assertion that *every singular matrix* $\mathbb{I} + \sqrt{3}\mathbf{n} \cdot \boldsymbol{\lambda}$ with $|\mathbf{n}| \leq 1$ is nonnegative.

Thus the cubic equation (14) and the quadratic restriction (15) together present a complete characterization of the ‘Bloch sphere’ $\partial\Omega_3$: *the boundary of Ω_3 is that portion of the cubic surface (Eq.14) contained within the unit ball $|\mathbf{n}| \leq 1$ in \mathbb{R}^8 . That $\partial\Omega_3$ is a closed surface was already clear from the fact that it is the boundary of a closed convex set in finite dimension.*

One might have noticed that the coefficients of the cubic terms in (14) exactly match the numerical values of the symmetric d_{jkl} symbols. Indeed, the quadratic and cubic terms in (14) equal respectively $3\mathbf{n} \cdot \mathbf{n}$ and $-2\mathbf{n} * \mathbf{n} \cdot \boldsymbol{\lambda}$. We may thus characterize the Bloch sphere

$\partial\Omega_3$ in a form which is as elegant as the characterization of CP^2 in Eq. (12):

$$\partial\Omega_3 = \{ \mathbf{n} \in \mathbb{R}^8 \mid 3\mathbf{n} \cdot \mathbf{n} - 2\mathbf{n} * \mathbf{n} \cdot \mathbf{n} = 1, \quad \mathbf{n} \cdot \mathbf{n} \leq 1 \}. \quad (17)$$

To go hand in hand with (12) and (17), the state space Ω_3 itself may be fully characterized in the following manner:

$$\Omega_3 = \{ \mathbf{n} \in \mathbb{R}^8 \mid 3\mathbf{n} \cdot \mathbf{n} - 2\mathbf{n} * \mathbf{n} \cdot \mathbf{n} \leq 1, \quad \mathbf{n} \cdot \mathbf{n} \leq 1 \}. \quad (18)$$

At the risk of repetition we stress that Ω_3 is a *portion* of the solid sphere in \mathbb{R}^8 . It is not $SO(8)$ invariant, but invariant under a 8-parameter subgroup thereof.

We have thus characterized Ω_3 and $\partial\Omega_3$ as compactly as Ω_3^{ext} in (12): $\partial\Omega_3$ corresponds to *saturation of one inequality*, the first one, in (18) while $\Omega_3^{\text{ext}} \subset \partial\Omega_3$ corresponds to *saturation of both*. That is, Ω_3^{ext} is that subset of $\partial\Omega_3$ for which $\mathbf{n} \cdot \mathbf{n} = 1$. These are the only two possibilities for saturation of the inequalities in (18), for the positivity condition $\rho(\mathbf{n}) \geq 0$ implies that under saturation of the second inequality the first one is automatically saturated. *This coordinate-free characterization is not only compact, but also renders $SU(3)$ invariance of Ω_3 , $\partial\Omega_3$, and Ω_3^{ext} manifest*, and is strictly analogous to

$$\begin{aligned} \Omega_2 &= B_3 = \{ \mathbf{n} \in \mathbb{R}^3 \mid \mathbf{n} \cdot \mathbf{n} \leq 1 \}, \\ \Omega_2^{\text{ext}} = \partial\Omega_2 &= S^2 = CP^1 = \{ \mathbf{n} \in \mathbb{R}^3 \mid \mathbf{n} \cdot \mathbf{n} = 1 \}, \end{aligned}$$

of the simpler case of two-dimensional Hilbert space.

C. Special spheres associated with Ω_3

As noted earlier, the boundary $\partial\Omega_3$ corresponds to singularity of the matrix $\mathbb{I} + \sqrt{3}\mathbf{n} \cdot \boldsymbol{\lambda}$, implying that the eigenvalues of the traceless matrix $\mathbf{n} \cdot \boldsymbol{\lambda}$ should necessarily be of the form

$$-\frac{1}{\sqrt{3}}, \quad \mu, \quad \frac{1}{\sqrt{3}} - \mu, \quad (19)$$

and nonnegativity of $\mathbb{I} + \sqrt{3}\mathbf{n} \cdot \boldsymbol{\lambda}$ is seen to restrict μ to the range given in (16), obtained earlier as consequence of $|\mathbf{n}| \leq 1$. Norm of $\mathbf{n} \in \mathbb{R}^8$ is determined by the eigenvalues of $\mathbf{n} \cdot \boldsymbol{\lambda}$, and we have

$$\begin{aligned} |\mathbf{n}| &\equiv \sqrt{\mathbf{n} \cdot \mathbf{n}} = \sqrt{\frac{1}{2} \text{tr}(\mathbf{n} \cdot \boldsymbol{\lambda})^2} \\ &= \sqrt{\frac{1}{2} \left[\left(\frac{1}{\sqrt{3}} \right)^2 + \mu^2 + \left(\frac{1}{\sqrt{3}} - \mu \right)^2 \right]}, \quad (20) \end{aligned}$$

whose minimum value is $1/2$ and corresponds to $\mu = (2\sqrt{3})^{-1}$. This value of μ is the ‘midpoint’ of the values $\mu = -\frac{1}{\sqrt{3}}, \frac{2}{\sqrt{3}}$ at which the maximum norm, $|\mathbf{n}| = 1$, obtains.

Thus the boundary $\partial\Omega_3$ can never stray into the interior of the eight-dimensional solid sphere of radius $1/2$ contained in Ω_3 . Since the maximum possible norm for \mathbf{n} is unity the boundary $\partial\Omega_3$, and hence the state space Ω_3 itself, can never stray into the exterior of the unit ball in \mathbb{R}^8 ; the latter result is a fact we knew all along.

Now, these two concentric balls in \mathbb{R}^8 of radii 1 and $1/2$ respectively are dual to one another in the following sense. The eigenvalues of $\mathbf{n} \cdot \boldsymbol{\lambda}$ corresponding to boundary points of Ω_3 falling on the outer sphere $|\mathbf{n}| = 1$ are $-\frac{1}{\sqrt{3}}, -\frac{1}{\sqrt{3}}, \frac{2}{\sqrt{3}}$ [irrespective of whether $\mu = -\frac{1}{\sqrt{3}}$ or $\frac{2}{\sqrt{3}}$] as may be seen from (19). But the eigenvalues of $\mathbf{n} \cdot \boldsymbol{\lambda}$ corresponding to boundary points on the inner sphere $|\mathbf{n}| = 1/2$ [i.e., $\mu = (2\sqrt{3})^{-1}$] are $\frac{1}{2\sqrt{3}}, \frac{1}{2\sqrt{3}}, -\frac{1}{\sqrt{3}}$. Thus, if $\mathbf{n} \in \mathbb{R}^8$ is a boundary point on the outer (unit) sphere (i.e., a pure state) then the opposite point of the inner sphere, $-\frac{1}{2}\mathbf{n}$, is definitely a boundary point too, and vice versa. In other words, *boundary points on the inner and outer spheres occur in dual pairs*. While the boundary points on the outer sphere correspond to vanishing von Neumann entropy, those on the inner sphere correspond to maximum entropy (one bit) among all boundary points.

There exists another special sphere ‘in between’ the inner and outer spheres which happens to be self-dual. Boundary points on this sphere corresponds to those $\mathbf{n} \in \mathbb{R}^8$ for which the matrix $\mathbf{n} \cdot \boldsymbol{\lambda}$ itself is singular (in addition to $\mathbb{I} + \sqrt{3}\mathbf{n} \cdot \boldsymbol{\lambda}$ being singular). We see from (19) that this situation corresponds to $\mu = 0$ or $\frac{1}{\sqrt{3}}$. Interestingly, the ‘midpoint’ of these two values, namely $(2\sqrt{3})^{-1}$, is the value of μ that defines the inner sphere. The eigenvalues of $\mathbf{n} \cdot \boldsymbol{\lambda}$ for such boundary points are clearly $\frac{1}{\sqrt{3}}, 0, -\frac{1}{\sqrt{3}}$, and so the norm $|\mathbf{n}| = 1/\sqrt{3}$. It is clear that if \mathbf{n} corresponds to such a boundary point on the sphere of radius $1/\sqrt{3}$ then the antipodal point $-\mathbf{n}$ too is a boundary point. In other words, *boundary points on the sphere of radius $1/\sqrt{3}$ obtain in pairs of diametrically opposite points*. It is in this sense that this sphere is self dual.

In our analysis of the two-sections to be taken up in the next Section, we shall come across sections of these three special eight-dimensional spheres.

IV. TWO-SECTIONS OF Ω_3

That Ω_3 and $\partial\Omega_3$ are substantially richer than the traditional Bloch ball and its boundary S^2 of a qubit is transparent. To obtain a feel for this richness it is sufficient to try the challenge of visualizing how the four-parameter family Ω_3^{ext} is ‘sprinkled’ over the seven-parameter surface $\partial\Omega_3$ of Ω_3 . It is in order to gain some insight into the geometry of this ‘Bloch sphere’ Ω_3 that we now move on to look at its two and three-dimensional sections.

A general two-section of Ω_3 should rightfully mean all

density operators of the form

$$\rho = \frac{1}{3} \left(\mathbb{I} + \alpha \tilde{\lambda}_1 + \beta \tilde{\lambda}_2 \right), \quad (21)$$

where $\tilde{\lambda}_1, \tilde{\lambda}_2$ is a pair of linearly independent traceless hermitian matrices, and α, β are real. Two-sections determined by $(\tilde{\lambda}_1, \tilde{\lambda}_2)$ and $(\tilde{\lambda}'_1, \tilde{\lambda}'_2)$ are unitarily equivalent if there exists $U \in SU(3)$ such that the real linear span of $(U\tilde{\lambda}_1U^\dagger, U\tilde{\lambda}_2U^\dagger)$ is the same as that of $(\tilde{\lambda}'_1, \tilde{\lambda}'_2)$. It is true that it suffices to consider only unitarily inequivalent two-sections, but the manifold of such two-sections is a huge family: for while we may choose without loss of generality $\tilde{\lambda}_1 = (\cos \theta \lambda_3 + \sin \theta \lambda_8)$, $\tilde{\lambda}_2$ is then left in the general form

$$\tilde{\lambda}_2 = (\sin \theta \lambda_3 - \cos \theta \lambda_8) + \sum_{j \neq 3, 8} r_j \lambda_j,$$

where j runs over all the six ‘off-diagonal’ λ -matrices. The unitarily inequivalent two-sections are thus parametrized by continuous real parameters θ, r_j (six in all, since one can be normalized away). In order to gain quick partial insight into the geometry of Ω_3 we consider here not general two-sections, but only standard two-sections, i.e. sections spanned by a pair of standard λ -matrices.

Such two-sections of the quantum state space have been considered earlier by other authors [6–10]. Yet we consider them here, briefly, for three reasons: (i) as preparation towards our detailed consideration of three-sections in the next Section; (ii) to point out the special significance of the circle of radius $1/\sqrt{3}$, and (iii) to examine the unitary equivalence or otherwise of geometrically equivalent sections.

Circle	Triangle	Parabola	Ellipse
12, 13, 23	18	34	48
14, 15, 16	28	35	58
17, 24, 25	38	36	68
26, 27, 45		37	78
46, 47, 56			
57, 67			

TABLE I: The 28 standard two-sections arranged according to their types, with jk denoting the section spanned by the λ -matrices (λ_j, λ_k) .

The ${}^8C_2 = 28$ two-sections of Ω_3 , the state space of qutrit, partition into four distinct families as shown in Table I. To exhibit the shape of each one of the two-sections it is sufficient to obtain an expression for its (closed) boundary, and this is obtained by restriction of the general expression for the closed boundary $\partial\Omega_3 \subset \mathbb{R}^8$, given in Eq. (14), to the two-section under consideration. Restriction to the (12) section gives

$$3(n_1^2 + n_2^2) = 1, \quad (22)$$

which is a circle of radius $1/\sqrt{3}$. Since pure states correspond to $|\mathbf{n}| = 1$, there is no pure state on this circle of

radius $1/\sqrt{3}$. Restriction of Eq. (14) to the (18) section gives

$$3(n_1^2 + n_8^2) - 6n_8 \left(n_1^2 - \frac{n_8^2}{3} \right) = 1, \quad (23)$$

which factors into the transparent form

$$(1 + n_8 + \sqrt{3}n_1)(1 + n_8 - \sqrt{3}n_1)(1 - 2n_8) = 0, \quad (24)$$

a triangle whose sides are decided by the vanishing of one of the three linear factors. The three vertices, the points at which two of the linear factors vanish simultaneously, are: $(n_1, n_8) = (0, -1), \frac{1}{2}(\pm\sqrt{3}, 1)$. Note that $|\mathbf{n}|^2 = n_1^2 + n_8^2 = 1$ for all three points, showing that these vertices correspond to pure states. The corresponding three Hilbert space vectors $|\psi\rangle$ are respectively $(0, 0, 1), (1, 0, 0), (0, 1, 0)$. Restriction of Eq. (14) to the (34) section yields

$$3(n_3^2 + n_4^2) - 3\sqrt{3}n_3n_4 = 1, \quad (25)$$

which factors into

$$(1 + \sqrt{3}n_3 - 3n_4^2)(1 - \sqrt{3}n_3) = 0, \quad (26)$$

a parabola $1 + \sqrt{3}n_3 = 3n_4^2$, truncated along the line $n_3 = 1/\sqrt{3}$, this line meeting the parabola at $(n_3, n_4) = (\frac{1}{\sqrt{3}}, \pm\sqrt{\frac{2}{3}})$. We find $|\mathbf{n}|^2 = n_3^2 + n_4^2 = 1$ at these two points, showing that these points correspond to pure states. The corresponding Hilbert space vectors $|\psi\rangle$ are $\frac{1}{\sqrt{3}}(\sqrt{2}, \pm 1)$. Finally, restriction of the general expression Eq. (14) for $\partial\Omega_3$ to the (48) section results in

$$3(n_4^2 + n_8^2) - 3n_8n_4^2 = 1, \quad (27)$$

which factors into

$$\left(3n_4^2 + 2 \left(n_8 + \frac{1}{4} \right)^2 - \frac{9}{8} \right) (1 + n_8) = 0, \quad (28)$$

an ellipse with major axis along the n_8 axis, semi-major axis $3/4$, semiminor axis $\sqrt{3}/8$, and centred at $(x_4, x_8) = (0, -1/4)$. The only pure state on this ellipse is at $(n_4, n_8) = (0, -1)$, the corresponding Hilbert space vector being $|\psi\rangle = (0, 0, 1)$

The two-sections thus assume one of the four closed convex shapes—triangle, (truncated) parabola, ellipse, or circle—exhibited in Fig. 1. While the first three have respectively 3, 2, 1 pure states, the last two-section has none. Since unitary transformations $\rho \rightarrow U\rho U^\dagger$, $U \in SU(3)$ are $SO(8)$ rotations on Ω_3 , unitarily equivalent sections are geometrically equivalent. But the converse is not necessarily true (not all $SO(8)$ rotations correspond to $SU(3)$ conjugation), and therefore we now turn to consideration of the issue of unitarily equivalent sections.

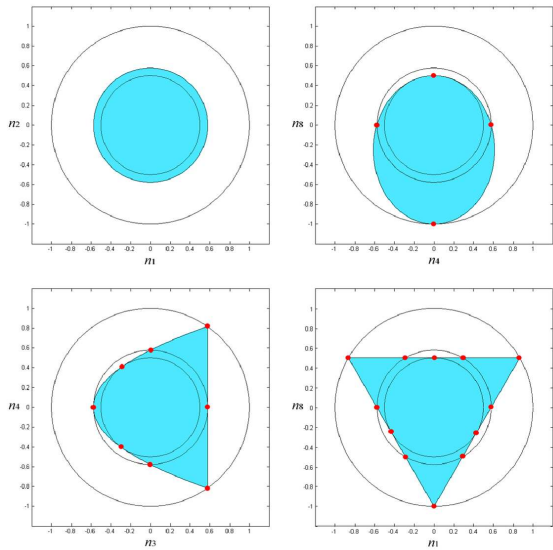


FIG. 1: Showing the four types of two-sections of Ω_3 . Shown also are circles of radii 1 , $1/\sqrt{3}$, and $1/2$ these being sections of the three special spheres discussed in Section 3C. The triangular, parabolic, and elliptic boundaries are seen to touch the ‘inner’ and ‘outer’ spheres at respectively three, two, and one dual pairs of points, and the ‘middle’ sphere at correspondingly equal number of self-dual pairs.

Unitary equivalence of the three triangular two-sections (18), (28), (38) is easily seen: conjugation by the unitary matrix $\exp(i\frac{\pi}{4}\lambda_j)$ takes λ_k to $\pm\lambda_l$ (this signature is of no consequence for our purposes) without affecting λ_8 . Here $jkl = 123$, or a permuted version thereof. Turning to the four parabolic two-sections, we see that conjugation by $U = \text{diag}(1, 1, i)$ takes λ_4 to λ_5 and λ_6 to λ_7 , leaving λ_3 invariant, thus establishing the unitary equivalences (34) \sim (35), (36) \sim (37). Conjugation by $\exp(i\frac{\pi}{2}\lambda_2)$ takes λ_4 to λ_6 and λ_5 to λ_7 leaving λ_3 essentially unaffected (actually λ_3 is transformed to $-\lambda_3$, but for our purpose on hand this is as good as λ_3 being left invariant), showing the unitary equivalences (34) \sim (36), (35) \sim (37), and thus demonstrating that the four parabolic sections are indeed unitarily equivalent to one another. Unitary equivalence of the four elliptic two-sections may be seen in *exactly* the same manner as the parabolic case.

The remaining seventeen two-sections are all circles of the same radius $1/\sqrt{3}$, as may be seen through restriction of Eq. (14). This by itself, however, does not prove their unitary equivalence, as noted earlier. Indeed, *these circular sections are not in the same unitary equivalence class*. And so this case deserves a more careful examination.

Note, first of all, that the (12), (13), and (23) sections are unitarily equivalent to one another, for $\exp(i\frac{\pi}{4}\lambda_j)$ leaves, under conjugation, λ_j invariant and rotates λ_k and λ_l . Here $jkl = 123$ or a permuted version of the same. Further, conjugation by $\exp(i\frac{\pi}{2}\lambda_7)$ takes λ_1, λ_2 to λ_4, λ_5 and that by $\exp(i\frac{\pi}{2}\lambda_5)$ takes λ_1, λ_2 to λ_6, λ_7 , showing the equivalences (12) \sim (45) \sim (67).

We have thus shown that the (12), (13), (23), (45), and (67) sections, forming a five-element subset, are unitarily equivalent to one another. Unitary equivalence of the remaining twelve elements (14), (15), (16), (17), (24), (25), (26), (27), (46), (47), (56), and (57) can be similarly seen using conjugation by one of the diagonal unitaries $\text{diag}(1, 1, i)$, $\text{diag}(1, i, 1)$, $\text{diag}(i, 1, 1)$ or one of $\exp(i\frac{\pi}{2}\lambda_2)$, $\exp(i\frac{\pi}{2}\lambda_5)$, $\exp(i\frac{\pi}{2}\lambda_7)$.

But these two subsets of circular two-sections form different unitary equivalence classes. To prove this it suffices to simply point out that *the first subset consists of anti-commuting pairs of λ -matrices, a property the second subset does not share*. Equivalently, $(\mathbf{n} \cdot \boldsymbol{\lambda})^2$ are simultaneously diagonal for all \mathbf{n} in the first case. But this is not true of the second class, since $(\mathbf{n} \cdot \boldsymbol{\lambda})^2$ for different \mathbf{n} ’s do not commute for this class.

The fact that there are two unitarily inequivalent classes of circular two-sections does not seem to have been appreciated in earlier considerations of two-sections [6–10].

Remark: Care should be exercised in comparing our results on two-sections with those of Kryszewski and Zachcial [10]. They have more than four rotationally inequivalent sections. The reason for this departure is not hard to see. They have made an unusual choice for normalization of their λ -matrices in that $\text{tr } \lambda_j^2$ is not the same for all values of j . As a consequence, the adjoint action $\rho \rightarrow U\rho U^\dagger$ of $U \in SU(3)$ does not act as rotation on their Ω_3 . This in turn forces the situation wherein unitarily equivalent two-sections are not necessarily rotationally equivalent!

In Fig.1 depicting the four geometrically different shapes of two-sections we have shown also the unit circle and the circles of radii $1/\sqrt{3}$, $1/2$. As was to be expected, the boundary of no two-section strays into the circle of radius $1/2$ or outside the unit circle. Further, if the boundary touches the circle of radius $1/2$ at some point, at the diametrically opposite point too it touches the unit circle. In other words, such boundary points always occur in dual pairs: there are three such dual pairs for the triangular section, two for the parabolic, one for the elliptic, and none for the circular section.

While the unit circle and the circle of radius $1/2$ are mutually dual in this sense, the circle of radius $1/\sqrt{3}$ is self-dual: if a point of this circle is a boundary point, its antipodal point will also be a boundary point. It can be seen that there are three such antipodal pairs for the triangular section, two for the parabolic, and one for the elliptic section; the entire circular section comprises, of course, only such pairs.

V. THREE-SECTIONS OF Ω_3

In the last Section we considered briefly the manner in which the 28 standard two-sections of Ω_3 get themselves organized into four families or geometric types. We shall now extend this analysis to the richer case of the ${}^8C_3 =$

56 standard three-sections. As will be seen below, there are seven geometrically distinct types of three-sections, and Table II shows the type to which each of these 56 sections belongs.

Sphere	Ellipsoid	Cone	Obese Tetrahedron	RS1	RS2	Paraboloid
123, 245	458	128	146	134	148	345
124, 246	468	138	157	135	158	367
125, 257	478	238	247	136	168	
126, 267	568	348	256	137	178	
127, 456	578	358	346	234	248	
145, 457	678	368	347	235	258	
147, 467		378	356	236	268	
156, 567			357	237	278	
167						

TABLE II: The 56 three-sections arranged according to their geometric types, jkl denoting the section spanned by $(\lambda_j, \lambda_k, \lambda_l)$.

In analyzing each type of three-sections we shall consider one member in some detail, display the density operators pertaining to the member, and then indicate *if and how* all the other members of the same geometric type are unitarily equivalent to the section considered. The three-sections spanned by $(\lambda_j, \lambda_k, \lambda_l)$ will be simply denoted (jkl) and, naturally, our strategy will be to take Eq. (14) describing the closed boundary $\partial\Omega_3$ of our Bloch ball Ω_3 and restrict it to the linear span of $(\lambda_j, \lambda_k, \lambda_l)$ to obtain a description of the closed boundary of the section (jkl) . We begin our analysis with the case of cone.

A. Cone

The particular three-section we shall consider for the conical type is (128), spanned by the triplet $(\lambda_1, \lambda_2, \lambda_8)$. Restriction of Eq. (14) to the three space (128) reads

$$3(n_1^2 + n_2^2 + n_8^2) - 6n_8 \left(n_1^2 + n_2^2 - \frac{n_8^2}{3} \right) = 1. \quad (29)$$

This equation readily factors into the suggestive form

$$((n_8 + 1)^2 - 3(n_1^2 + n_2^2)) (2n_8 - 1) = 0, \quad (30)$$

which is clearly a cone with vertex at $(n_1, n_2, n_8) = (0, 0, -1)$, truncated by the base plane $n_8 = 1/2$, as shown in Fig.2. There is a singleton pure state at $(0, 0, -1)$ and a circle of pure states at $n_8 = 1/2$, $\sqrt{n_1^2 + n_2^2} = \sqrt{3}/2$; these are the points at which the cone touches the outer sphere (unit sphere).

Clearly, the density operators belonging to this three-section are of the form

$$\rho = \frac{1}{3} \begin{pmatrix} 1 + n_8 & \sqrt{3}(n_1 - in_2) & 0 \\ \sqrt{3}(n_1 + in_2) & 1 - n_8 & 0 \\ 0 & 0 & 1 - 2n_8 \end{pmatrix}, \quad (31)$$

which can be verified to be positive if and only if the three-vector $\mathbf{n} = (n_1, n_2, n_8)$ is in this (truncated) solid

cone [here, as in the rest of this Section, three-component vectors like $\mathbf{n} = (n_1, n_2, n_8)$ will always refer to the corresponding $\mathbf{n} = (n_1, 0, 0, n_2, 0, 0, n_8, 0, 0) \in \mathbb{R}^8$].

And it can be seen that the singleton and circle of pure states correspond respectively to Hilbert space unit vectors $|\psi\rangle = (0, 0, 1)$ and $\frac{1}{\sqrt{2}}(1, e^{i\theta}, 0)$.

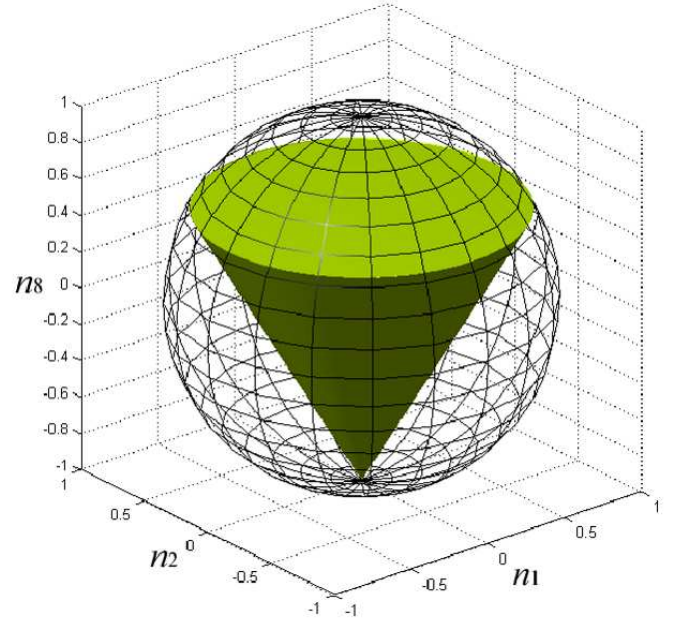


FIG. 2: Showing the conical (128) three-section having a singleton pure state at its vertex and a circle of pure states at its base.

That the seven three-sections listed under ‘cone’ in Table II are unitarily equivalent to one another is particularly easy to see. Conjugation by $\exp(i\frac{\pi}{4}\lambda_1)$ leaves λ_1, λ_8 invariant but transforms λ_2 to λ_3 , demonstrating the unitary equivalence $(128) \sim (138)$. Similarly, the equivalence $(138) \sim (238)$ is established by $\exp(i\frac{\pi}{4}\lambda_3)$. The equivalence $(138) \sim (348)$ is seen by noting that conjugation by the unitary permutation matrix

$$U = \begin{pmatrix} 0 & 1 & 0 \\ 0 & 0 & 1 \\ 1 & 0 & 0 \end{pmatrix} \quad (32)$$

takes λ_1 to λ_4 and the linear span of (λ_3, λ_8) onto itself. Finally, the equivalences $(348) \sim (358)$ and $(368) \sim (378)$ are established by the diagonal unitary matrix $\text{diag}(1, 1, i)$, while $(348) \sim (368)$, $(358) \sim (378)$ are witnessed by $\exp(i\frac{\pi}{2}\lambda_2)$.

B. Paraboloid

C. Ellipsoid

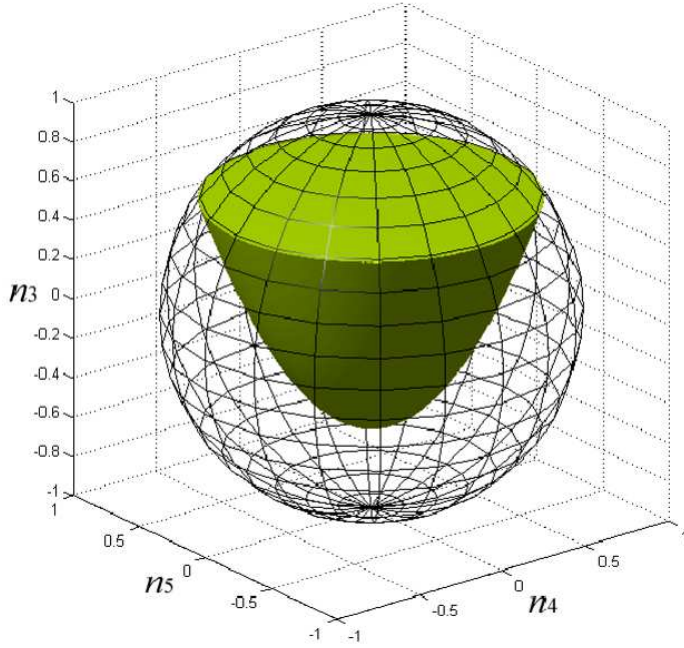


FIG. 3: Showing the paraboloidal three-section (345) having a circle of pure states

The three-sections (345) and (367) alone belong to the paraboloid type. Restriction of Eq. (14) to the (345) case reads

$$3(n_3^2 + n_4^2 + n_5^2) - 3\sqrt{3}n_3(n_4^2 + n_5^2) = 1, \quad (33)$$

which conveniently factors into

$$(1 - \sqrt{3}n_3) \left(3(n_4^2 + n_5^2) - (\sqrt{3}n_3 + 1) \right) = 0. \quad (34)$$

The closed boundary of the three-section (345) is thus seen to be the paraboloid $3(n_4^2 + n_5^2) = \sqrt{3}n_3 + 1$ truncated by the plane $n_3 = 1/\sqrt{3}$, the latter acting as the ‘closing lid’, as shown in Fig. 3. This three-section has a circle worth of pure states and these correspond to $n_3 = 1/\sqrt{3}$, $n_4^2 + n_5^2 = 2/3$, the points at which the paraboloid touches the outer sphere. The density operators corresponding to this section necessarily have the form

$$\rho = \frac{1}{3} \begin{pmatrix} 1 + \sqrt{3}n_3 & 0 & \sqrt{3}(n_4 - in_5) \\ 0 & 1 - \sqrt{3}n_3 & 0 \\ \sqrt{3}(n_4 + in_5) & 0 & 1 \end{pmatrix}, \quad (35)$$

and we see that positivity of ρ is indeed equivalent to the three-vector $\mathbf{n} = (n_3, n_4, n_5)$ being in the solid (truncated) paraboloidal region of Fig. 3. The circle worth of pure states correspond to Hilbert space vectors $|\psi\rangle = \frac{1}{\sqrt{3}}(\sqrt{2}, 0, e^{i\theta})$, $0 \leq \theta < 2\pi$. Finally the fact that the three-sections (345) and (367) are unitarily equivalent may be seen through conjugation by $\exp(i\frac{\pi}{2}\lambda_2)$.

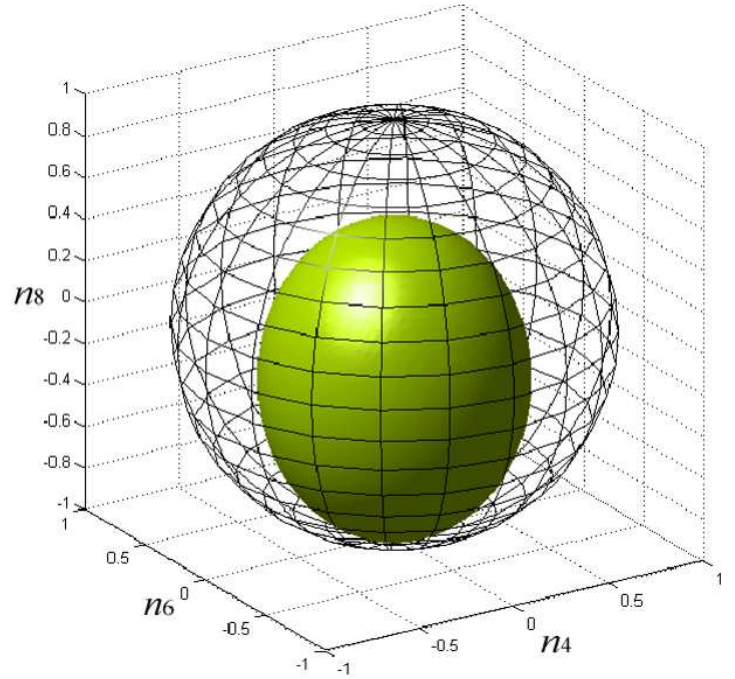


FIG. 4: Showing the ellipsoidal (468) three-section having only one pure state

As may be seen from Table II, there are six three-sections of this type, and we begin with the specific case of (468). Restriction of Eq. (14) to this case reads

$$3(n_4^2 + n_6^2 + n_8^2) + n_8(3n_4^2 + 3n_6^2 + 2n_8^2) = 1. \quad (36)$$

This cubic expression factorizes, as in the previous two cases, into

$$(1 + n_8) \left(3(n_4^2 + n_6^2) + 2 \left(n_8 + \frac{1}{4} \right)^2 - \frac{9}{8} \right) = 0. \quad (37)$$

This is clearly an ellipsoid of revolution (about the major axis n_8), with semimajor axis $3/4$ and semiminor axis $\sqrt{3}/8$, with the centre of the ellipsoid located at $(n_4, n_6, n_8) = (0, 0, -1/4)$. It touches the outer sphere only at the point $(0, 0, -1)$, as seen also from Fig. 4 and hence there is only one pure state in this three-section. As expected, the boundary touches the inner sphere at the dual point $(0, 0, 1/2)$ and only at this point. Any density operator that belongs to the (468) section has to have the form

$$\rho = \frac{1}{3} \begin{pmatrix} 1 + n_8 & 0 & \sqrt{3}n_4 \\ 0 & 1 + n_8 & \sqrt{3}n_6 \\ \sqrt{3}n_4 & \sqrt{3}n_6 & 1 - 2n_8 \end{pmatrix}, \quad (38)$$

and we see that $\rho \geq 0$ if and only if the three-vector $\mathbf{n} = (n_4, n_6, n_8)$ lies in this solid ellipsoid. The singleton pure state is seen to correspond to Hilbert space vector $|\psi\rangle = (0, 0, 1)$.

The four components n_4, n_5, n_6, n_7 of \mathbf{n} enters the relevant part of Eq. (14) *symmetrically*, and only in the combination $n_4^2 + n_5^2 + n_6^2 + n_7^2$. It follows that all the six three-sections listed under ‘ellipsoid’ in Table II will have identical geometric structure, for they are obtained by simply picking two out of these four components to partner with n_8 . However, while unitary equivalence of two three-sections implies their geometric equivalence, the converse is not true in general, and so we explore this issue.

Unitary equivalence of (468) and (478) is established through the diagonal unitary $\text{diag}(1, i, 1)$. The same is true of the equivalence (578) \sim (568) as well. And the unitary equivalence (468) \sim (578) is established through the unitary $\text{diag}(1, 1, i)$. Thus, the sections (468), (478), (578), and (568) are unitarily equivalent to one another. Similarly (458), (678) is a pair of unitarily equivalent sections, as may be seen through conjugation by $\exp(i\frac{\pi}{2}\lambda_2)$. *These two subsets are, however, unitarily inequivalent.* Proof consists in simply noting that λ_4, λ_5 (as also λ_6, λ_7) anticommute, but there exists no such pair in the (real) linear span of $\lambda_4, \lambda_6, \lambda_8$.

D. Obese-tetrahedron

The conical, paraboloidal, and ellipsoidal three-sections considered so far are related respectively to the triangular, parabolic, and elliptical two-sections of the previous Section in an obvious manner. It is for this reason that the cubic expression forming the left hand side of Eq. (14) factorized into a quadratic and a linear expression in these three cases. It turns out that the next three types of three-sections are genuinely cubic.

There are eight three-sections of the obese-tetrahedral type as shown in Table II, and we begin with the case of (146). Restriction of Eq. (14) which describes the boundary of Ω_3 to the present case gives the following equation for the boundary of the (146) section:

$$3(n_1^2 + n_4^2 + n_6^2) - 6\sqrt{3}n_1n_4n_6 = 1. \quad (39)$$

Unlike the previous three cases, this expression does not factorize: the boundary of this three-section is genuinely cubic. For reasons which will become clear later on, we call this three dimensional solid, shown in Fig. 5, the *obese-tetrahedron*.

This section has four, and only four, pure states, the points at which the obese-tetrahedron touches the outer sphere. These are

$$(n_1, n_4, n_6) = \begin{aligned} & \frac{1}{\sqrt{3}}(1, 1, 1), \quad \frac{1}{\sqrt{3}}(1, -1, -1), \\ & \frac{1}{\sqrt{3}}(-1, 1, -1), \quad \frac{1}{\sqrt{3}}(-1, -1, 1). \end{aligned} \quad (40)$$

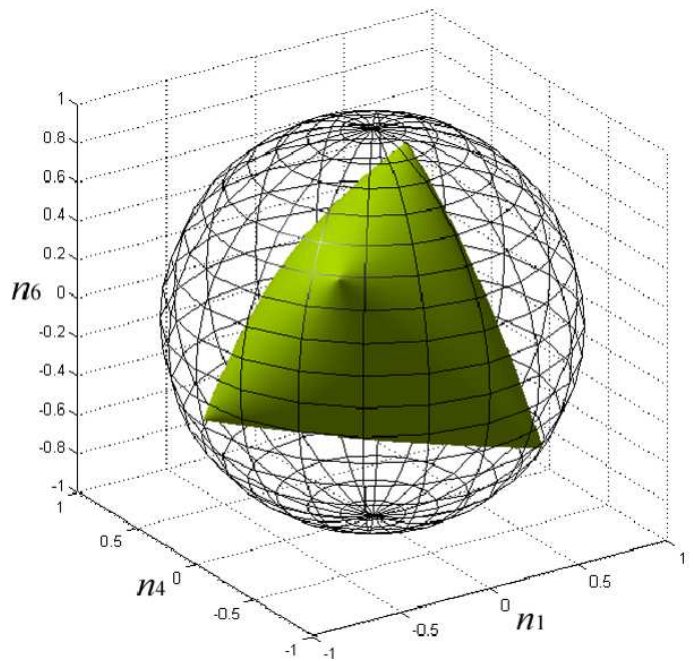


FIG. 5: Showing the obese-tetrahedral three-section(146) having four pure states

The density operators corresponding to this section necessarily assume the form

$$\rho = \frac{1}{3} \begin{pmatrix} 1 & \sqrt{3}n_1 & \sqrt{3}n_4 \\ \sqrt{3}n_1 & 1 & \sqrt{3}n_6 \\ \sqrt{3}n_4 & \sqrt{3}n_6 & 1 \end{pmatrix}, \quad (41)$$

which is verified to be positive if and only if $\mathbf{n} = (n_1, n_4, n_6)$ is a point in the obese tetrahedron shown in Fig. 5. It is readily seen that Hilbert space vectors $|\psi\rangle$ corresponding to the above four pure states are, respectively, $\frac{1}{\sqrt{3}}(1, 1, 1)$, $\frac{1}{\sqrt{3}}(1, 1, -1)$, $\frac{1}{\sqrt{3}}(1, -1, 1)$, $\frac{1}{\sqrt{3}}(-1, 1, 1)$.

Unitary equivalence of the eight obese-tetrahedral sections can be seen as follows. The unitary equivalences (146) \sim (157), (146) \sim (247), and (146) \sim (256) are seen through conjugation by $\text{diag}(1, 1, i)$, $\text{diag}(1, i, 1)$, and $\text{diag}(i, 1, 1)$ respectively, showing that the four sections (146), (157), (247), (256) are unitarily equivalent to one another. Similarly, the unitary equivalences (346) \sim (347), (346) \sim (356), and (346) \sim (357) are seen through conjugation by $\text{diag}(1, i, 1)$, $\text{diag}(i, 1, 1)$ and $\text{diag}(1, 1, i)$ respectively, showing that the four sections (346), (347), (356), (357) are unitarily equivalent to one another. Finally, the unitary equivalence (146) \sim (346) is seen through conjugation by $\exp(i\frac{\pi}{4}\lambda_2)$ which takes λ_1 to λ_3 , leaving invariant the linear span of (λ_4, λ_6) . This completes proof of unitary equivalence of the eight obese-tetrahedral three-sections to one another.

The next two types to be considered also turn out to be genuine cubic sections. Since these two shapes are un-

familiar, at least to the present authors, these two three-sections will be simply denoted RS1 and RS2.

E. RS1

As may be seen from Table II there are eight three-sections of type RS1. We consider first the section (134). Restriction of Eq. (14) to (134) reads

$$3(n_1^2 + n_3^2 + n_4^2) - 3\sqrt{3}n_4^2n_3 = 1, \quad (42)$$

giving the boundary of RS1 shown in Fig. 6. It is to be appreciated that the signature in front of $3\sqrt{3}n_4^2n_3$ has no effect on the shape of the section, for it can be simply absorbed into n_3 . This section has just two pure states, represented by the pair of points $(n_1, n_3, n_4) = (0, \frac{1}{\sqrt{3}}, \pm \frac{2}{\sqrt{3}})$ at which RS1 touches the unit sphere. It is clear that these two pure states correspond to Hilbert space vectors $|\psi\rangle = (\sqrt{2}, 0, \pm 1)/\sqrt{3}$.

The density operators of this section have to be of the form

$$\rho = \frac{1}{3} \begin{pmatrix} 1 + \sqrt{3}n_3 & \sqrt{3}n_1 & \sqrt{3}n_4 \\ \sqrt{3}n_1 & 1 - \sqrt{3}n_3 & 0 \\ \sqrt{3}n_4 & 0 & 1 \end{pmatrix}, \quad (43)$$

which is easily verified to be positive if and only if the condition $3(n_1^2 + n_3^2 + n_4^2) - 3\sqrt{3}n_4^2n_3 \leq 1$ is met, i.e., if and only if $\mathbf{n} = (n_1, n_3, n_4) \in \text{RS1}$.

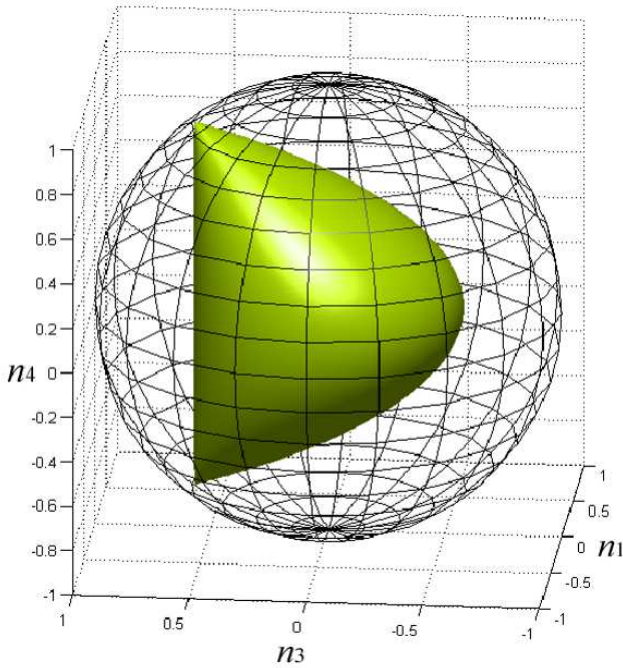


FIG. 6: Showing the RS1 three-section (134) having two pure states.

Unitary equivalence of the eight sections of type RS1 can be seen as follows. That (134) \sim (135) follows from conjugation by $\text{diag}(1, 1, i)$, and (136) \sim (137) follows from the same conjugation. The equivalences (134) \sim (136), (135) \sim (137) follow from conjugation by $\exp(i\frac{\pi}{2}\lambda_2)$, thus proving the equivalence of (134), (135), (136), (137) to one another.

The equivalence (234) \sim (235) follows from conjugation by $\text{diag}(1, 1, i)$, and the same conjugation establishes also the equivalence (236) \sim (237). The equivalences (234) \sim (236), (235) \sim (237) are seen through conjugation by $\exp(i\frac{\pi}{2}\lambda_2)$, thus proving equivalence of (234), (235), (236), (237) to one another.

Finally, the equivalences (134) \sim (234) and (135) \sim (235) are seen through conjugation by $\text{diag}(1, i, 1)$, and the equivalences (136) \sim (236) and (137) \sim (237) through conjugation by $\text{diag}(i, 1, 1)$, thus establishing unitary equivalence of the eight three-sections of type RS1.

F. RS2

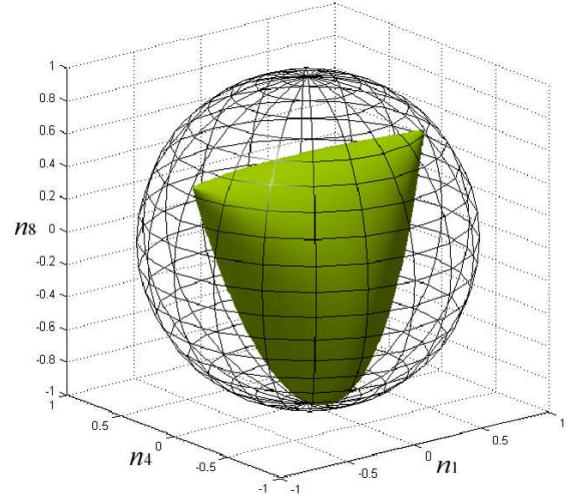


FIG. 7: Showing the three-section (148) of type RS2, having three pure states

There are eight three-sections of this type, and these are listed in Table II. We begin with the section (148). Restriction of Eq. (14) to this section reads

$$3(n_1^2 + n_4^2 + n_8^2) - 3n_8 \left(2n_1^2 - n_4^2 - \frac{2}{3}n_8^2 \right) = 1, \quad (44)$$

giving the boundary of RS2 shown in Fig. 7. This section has three pure states corresponding to the points $(n_1, n_4, n_8) = (0, 0, -1)$, $(\pm \frac{\sqrt{3}}{2}, 0, \frac{1}{2})$ at which RS2

touches the unit sphere. Hilbert space vectors $|\psi\rangle$ corresponding to these three pure states are readily seen to be $(0, 0, 1)$, $\frac{1}{\sqrt{2}}(1, \pm 1, 0)$.

The density operators which correspond to this section necessarily assume the form

$$\rho = \frac{1}{3} \begin{pmatrix} 1 + n_8 & \sqrt{3}n_1 & \sqrt{3}n_4 \\ \sqrt{3}n_1 & 1 + n_8 & 0 \\ \sqrt{3}n_4 & 0 & 1 - 2n_8 \end{pmatrix}, \quad (45)$$

whose positivity indeed demands $3(n_1^2 + n_4^2 + n_8^2) - 3n_8(2n_1^2 - n_4^2 - \frac{2}{3}n_8^2) \leq 1$, i.e. that $\mathbf{n} = (n_1, n_4, n_8)$ be in RS2.

Proof of unitary equivalence of the eight sections of this type follows in exactly the same way it did in the case of RS1. It suffices to note that (1) these eight sections of type RS2 are obtained from the respective eight sections of type RS1 by simply replacing λ_3 with λ_8 , and (2) that every unitary used for conjugation towards proof of unitary equivalence in the case of RS1 mapped λ_3 to itself, and it has no effect on λ_8 too.

G. Sphere

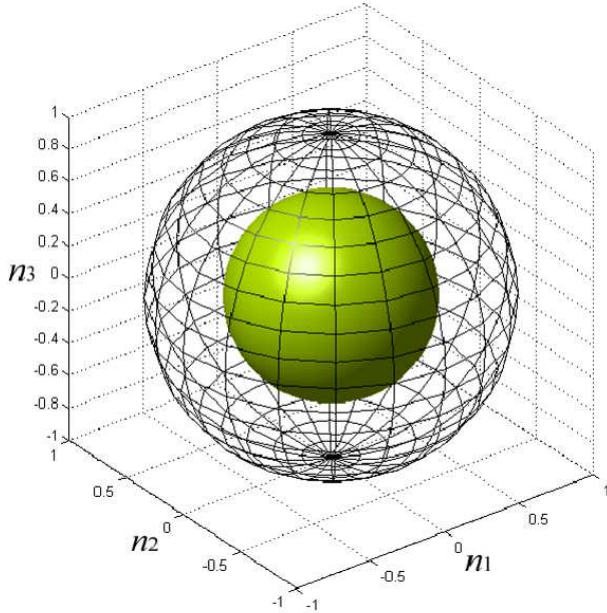


FIG. 8: Showing the (123) three-section which is spherical, having no pure states

As many as seventeen three-sections of Ω_3 are of this type. These are precisely the three-sections for which the restriction of Eq. (14) becomes purely quadratic. Thus, none of these sections involve λ_8 . They tend to avoid λ_3 as well, with the exception of the combination (123)

which does not enter the cubic part of Eq. (14). Further, (146), (157), (256), and (147) which involve neither λ_3 nor λ_8 do not belong to this type, but to the obese-tetrahedral case. Thus of the ${}^6C_3 = 20$ three-sections involving neither λ_3 nor λ_8 we remove the above four obese-tetrahedral sections, and add the exceptional case of (123) to arrive at seventeen.

Since the cubic terms of Eq. (15) contribute to none of these sections, restriction of Eq. (14) to section (jkl) of this type reads

$$3(n_j^2 + n_k^2 + n_l^2) = 1, \quad (46)$$

a sphere of radius $1/\sqrt{3}$, as shown in Fig. 8. It is the three-section of minimum 3-volume, not only among the standard three-sections, but among all three-sections. It is the only type which has no pure states.

These seventeen geometrically equivalent three-sections are *not unitarily equivalent to one another*. They can be grouped into three subsets. The section (123) is a singleton set in itself, for we know that $\lambda_1, \lambda_2, \lambda_3$ have the algebraic (commutation, anticommutation) properties which are similar to those of the Pauli matrices, and there is no other triplet among the λ -matrices which has this property.

Similarly we know that the three ‘imaginary’ λ -matrices $\lambda_2, \lambda_5, \lambda_7$ are $SO(3)$ generators. The triplets $(\lambda_1, \lambda_4, \lambda_7)$, $(\lambda_1, \lambda_5, \lambda_6)$, and $(\lambda_2, \lambda_4, \lambda_6)$ are related to the triplet $(\lambda_2, \lambda_5, \lambda_7)$ through conjugations by diagonal unitaries. And there is no other triplet among the λ -matrices which possess this structure of $SO(3)$ generators. So these four triplets form a second subset of unitarily equivalent three-sections.

Finally, the three *four-sections* (1245), (1267), and (4567) form spheres of radius $1/\sqrt{3}$, as may be seen from restriction of Eq. (14); *there exists no other four-section with this property*. These three *four-sections* are unitarily equivalent to one another: the equivalence $(1245) \sim (1267)$ is seen through conjugation by $\exp(i\frac{\pi}{2}\lambda_2)$ and the equivalence $(1267) \sim (4567)$ by $\exp(i\frac{\pi}{2}\lambda_7)$. Each one of these spherical four-sections leads to four spherical three-sections, adding to twelve. That these twelve spherical three-sections forming the third and last subset are unitarily equivalent to one another is thus established. *There are thus three unitarily inequivalent sets of spherical three-sections.*

H. Comparison with the work of Mendas

The 56 three-sections of Ω_3 , the state space of the qutrit, were earlier studied by Mendas [8] using *Monte Carlo sampling* method, leading to the conclusion that there are *ten* distinct types of three-sections. In contrast our approach is *analytic* and hence conclusive, and we have shown that there are only *seven* types. Further, we have presented for each type analytic expression for the three-section, and this was not possible in the Monte

Carlo approach. Finally, we have shown, both in the ellipsoidal and spherical cases, that there are three-sections which are geometrically the same but nevertheless are unitarily inequivalent, an aspect which is clearly beyond the purview of the Monte Carlo approach. The findings of Mendas [8] group all the six ellipsoidal sections into one ‘type’ (Type 10 of Mendas) and all the seventeen spherical three-sections into one type (Type 1); it groups the eight conical sections into three types (Types 2, 8, 9) and the eight obese-tetrahedral sections into two types (Types 4, 7), but now we know that all the eight conical sections are mutually equivalent not only geometrically but also unitarily. We have shown also that the same is true of the eight obese-tetrahedral sections as well.

VI. OBESSE-TETRAHEDRON: A DEEPER LOOK

In this Section we examine in more detail the interesting case of obese-tetrahedral three-sections. To be specific we consider again the (146) section. Several questions may arise from the very name, ‘obese’ and ‘tetrahedron’: (1) Do these three-sections really possess the full tetrahedral symmetry T_d familiar from the context of point groups? (2) If the answer is in the affirmative, where does this symmetry originate from? And, finally, (3) what forces the tetrahedron to be obese?

We begin with the last question. That a *tetrahedral section of Ω_3 has to necessarily be obese* can be traced to the very geometry of Ω_3 . We have already noted that a boundary point of Ω_3 which is closest to the origin can be no nearer than a distance of $1/2$, the radius of the inner-ball, and that such a nearest point will always be directly opposite to a pure state (and we know that the latter is at unit distance from the origin). Now in a tetrahedron with vertices on the outer (unit) sphere, points closest to the origin are at a distance $1/3$; there are four such points, the centres of the four faces of the tetrahedron. Thus *our tetrahedron is obese by the minimal amount so that these four ‘base points’ of the tetrahedron at a distance $1/3$ from the origin move away to $1/2$, just sufficient to fit the geometry of Ω_3 .*

The first two questions turn out to be connected, and so they are best treated together. Recall that the obese-tetrahedral (146) section consists of all 3×3 density matrices which are *real with equal entries along the diagonal*. We ask: what are the $SU(3)$ matrices U which under conjugation $\rho(\mathbf{n}) \rightarrow \rho'(\mathbf{n}) = \rho(\mathbf{n}') = U\rho(\mathbf{n})U^\dagger$ maps the (146) section onto itself. Such matrices will of course constitute a subgroup of $SU(3)$ and, indeed, it will be a subgroup of $SO(3) \subset SU(3)$. Since the relevant $SU(3)$ matrices are real, they will map the (257) three-section, the real linear span of the ‘imaginary’ λ -matrices onto itself. It follows that the (38) two-section of diagonal λ -matrices too will be mapped onto itself under the conjugation action of these matrices $\in SO(3) \subset SU(3)$. *This implies that the relevant $SO(3)$ matrices have to be signed or generalized permutation matrices.*

It is well known that every $SU(3)$ matrix acts on the eight λ -matrices, through conjugation, as an $SO(8)$ rotation; this is the adjoint representation of $SU(3)$. Thus, our consideration in the above paragraph shows that the question of what is the subgroup of $SU(3)$ which maps the (146) section in \mathbb{R}^8 onto itself is the same as the following question: What is the (maximal) subgroup of $SU(3)$ matrices whose adjoint representation has the form of a direct sum $3 \oplus 3 \oplus 2$, the two three-spaces arising as the linear spans (146), (256) respectively, and the two-space arising as the linear span (38)? This subgroup of real $SU(3)$ matrices is easily determined and it has 24 elements: the six 3×3 permutation matrices have *three* nonzero entries each; choice of independent signature for each entry results in $6 \times 2^3 = 48$ matrices, exactly half of them have positive determinant and hence are elements of $SO(3)$. This 24-element discrete subgroup of $SO(3)$ turns out to be *isomorphic to the tetrahedral group T_d* whose character table is reproduced in Table III.

T_d	$[e]$	$8[C_3]$	$3[C_2]$	$6[S_4]$	$6[\sigma_d]$
A_1	1	1	1	1	1
A_2	1	1	1	-1	-1
E	2	-1	2	0	0
T_1	3	0	-1	1	-1
T_2	3	0	-1	-1	1

TABLE III: Showing the character table of the tetrahedral point group T_d

We enumerate the elements of this discrete subgroup of $SO(3) \subset SU(3)$ in the same traditional order in which they are listed in the character table, namely identity, followed by the eight C_3 rotations, followed by the three C_2 rotations, followed by the six S_4 improper rotations, and finally the six mirror reflections.

Identity :

$$\begin{pmatrix} 1 & 0 & 0 \\ 0 & 1 & 0 \\ 0 & 0 & 1 \end{pmatrix},$$

C_3 Rotations :

$$\begin{pmatrix} 0 & 1 & 0 \\ 0 & 0 & 1 \\ 1 & 0 & 0 \end{pmatrix}, \begin{pmatrix} 0 & 1 & 0 \\ 0 & 0 & -1 \\ -1 & 0 & 0 \end{pmatrix}, \begin{pmatrix} 0 & -1 & 0 \\ 0 & 0 & -1 \\ 1 & 0 & 0 \end{pmatrix},$$

$$\begin{pmatrix} 0 & -1 & 0 \\ 0 & 0 & 1 \\ -1 & 0 & 0 \end{pmatrix}, \begin{pmatrix} 0 & 0 & 1 \\ 1 & 0 & 0 \\ 0 & 1 & 0 \end{pmatrix}, \begin{pmatrix} 0 & 0 & 1 \\ -1 & 0 & 0 \\ 0 & -1 & 0 \end{pmatrix},$$

$$\begin{pmatrix} 0 & 0 & -1 \\ -1 & 0 & 0 \\ 0 & 1 & 0 \end{pmatrix}, \begin{pmatrix} 0 & 0 & -1 \\ 1 & 0 & 0 \\ 0 & -1 & 0 \end{pmatrix}$$

C_2 Rotations :

$$\begin{pmatrix} 1 & 0 & 0 \\ 0 & -1 & 0 \\ 0 & 0 & -1 \end{pmatrix}, \begin{pmatrix} -1 & 0 & 0 \\ 0 & -1 & 0 \\ 0 & 0 & 1 \end{pmatrix}, \begin{pmatrix} -1 & 0 & 0 \\ 0 & 1 & 0 \\ 0 & 0 & -1 \end{pmatrix}$$

Improper rotations S_4 :

$$\begin{pmatrix} 1 & 0 & 0 \\ 0 & 0 & 1 \\ 0 & -1 & 0 \end{pmatrix}, \begin{pmatrix} 1 & 0 & 0 \\ 0 & 0 & -1 \\ 0 & 1 & 0 \end{pmatrix}, \begin{pmatrix} 0 & -1 & 0 \\ 1 & 0 & 0 \\ 0 & 0 & 1 \end{pmatrix},$$

$$\begin{pmatrix} 0 & 1 & 0 \\ -1 & 0 & 0 \\ 0 & 0 & 1 \end{pmatrix}, \begin{pmatrix} 0 & 0 & -1 \\ 0 & 1 & 0 \\ 1 & 0 & 0 \end{pmatrix}, \begin{pmatrix} 0 & 0 & 1 \\ 0 & 1 & 0 \\ -1 & 0 & 0 \end{pmatrix}$$

Mirror reflections σ_d :

$$\begin{pmatrix} -1 & 0 & 0 \\ 0 & 0 & -1 \\ 0 & -1 & 0 \end{pmatrix}, \begin{pmatrix} -1 & 0 & 0 \\ 0 & 0 & 1 \\ 0 & 1 & 0 \end{pmatrix}, \begin{pmatrix} 0 & -1 & 0 \\ -1 & 0 & 0 \\ 0 & 0 & -1 \end{pmatrix},$$

$$\begin{pmatrix} 0 & 1 & 0 \\ 1 & 0 & 0 \\ 0 & 0 & -1 \end{pmatrix}, \begin{pmatrix} 0 & 0 & -1 \\ 0 & -1 & 0 \\ -1 & 0 & 0 \end{pmatrix}, \begin{pmatrix} 0 & 0 & 1 \\ 0 & -1 & 0 \\ 1 & 0 & 0 \end{pmatrix}$$

We note that all these 24 matrices are signed permutation matrices, also called generalized permutation matrices. They all have unit determinant, since we insisted that they be elements of $SO(3)$ and not $O(3)$. If this requirement is relaxed, we get ‘another copy’ of 24 matrices, obtained by multiplying the original 24 by the negative of the unit matrix, namely $-\mathbb{I}$, adding to a total of 48. Noting that $-\mathbb{I}$ commutes with all elements, we recall the manner in which one goes, in the case of point groups, from the 24 element tetrahedral group T_d to the 48 element octahedral group O_h by simply adding a new element ‘inversion’ which commutes with all elements of T_d . Indeed, the full set of all 48 signed permutation matrices, with both signatures allowed for the determinant, is isomorphic to O_h . But this larger group is of no direct relevance for our present situation.

Remark: At the risk of repetition we note that the matrices above which go under ‘improper rotations S_4 ’ and ‘mirror reflections σ_d ’ are actually proper $SO(3)$ rotations. It is in anticipation of their action on certain three-sections of Ω_3 that we have so named them.

We have seen that the eight-dimensional real linear span of the λ -matrices decomposes, under the conjugation action of our tetrahedral group of twenty four $SO(3)$ matrices, into a direct sum of three (irreducible) orthogonal subspaces. In each subspace we will, therefore, expect to obtain a representation of T_d . It is instructive to actually construct these representations.

To this end let us relabel the eight λ -matrices as $\mathbf{J} = (J_1, J_2, J_3) \equiv (\lambda_2, \lambda_5, \lambda_7)$, $\mathbf{X} = (X_1, X_2, X_3) \equiv (\lambda_1, \lambda_4, \lambda_6)$, and $\mathbf{Q} = (Q_1, Q_2) = (\lambda_3, \lambda_8)$. Let us denote by R a generic element of our tetrahedral group $T_d \subset SO(3) \subset SU(3)$ of signed permutation matrices, and let the 8×8 matrix $\text{Ad}(R)$ be the image of R in the adjoint representation. With $\mathbf{x} = (x_1, x_2, x_3)$, $\mathbf{y} = (y_1, y_2, y_3) \in \mathbb{R}^3$ and $\mathbf{z} = (z_1, z_2) \in \mathbb{R}^2$, an element in the (real) linear span of the λ -matrices, which necessarily has the form $\mathbf{x} \cdot \mathbf{X} + \mathbf{y} \cdot \mathbf{J} + \mathbf{z} \cdot \mathbf{Q}$ with uniquely determined $\mathbf{x}, \mathbf{y}, \mathbf{z}$, can be denoted $\mathbf{n} = \mathbf{x} \oplus \mathbf{y} \oplus \mathbf{z} \in \mathbb{R}^8$. The point being made is that the 24 eight-dimensional matrices representing action of our group $T_d \subset SO(3) \subset SU(3)$ on \mathbb{R}^8 [the adjoint representation of $SU(3)$] simultaneously assume a direct sum form. That is, for every $R \in T_d$

$$\begin{aligned} \mathbf{x} \cdot \mathbf{X} + \mathbf{y} \cdot \mathbf{J} + \mathbf{z} \cdot \mathbf{Q} &\rightarrow R(\mathbf{x} \cdot \mathbf{X} + \mathbf{y} \cdot \mathbf{J} + \mathbf{z} \cdot \mathbf{Q})R^T \\ &= \mathbf{x}' \cdot \mathbf{X} + \mathbf{y}' \cdot \mathbf{J} + \mathbf{z}' \cdot \mathbf{Q}, \end{aligned}$$

with

$$\begin{aligned} \mathbf{y}' \cdot \mathbf{J} &= R(\mathbf{y} \cdot \mathbf{J})R^T = (T_1(R)\mathbf{y}) \cdot \mathbf{J}, \\ \mathbf{x}' \cdot \mathbf{X} &= R(\mathbf{x} \cdot \mathbf{X})R^T = (T_2(R)\mathbf{x}) \cdot \mathbf{X}, \\ \mathbf{z}' \cdot \mathbf{Q} &= R(\mathbf{z} \cdot \mathbf{Q})R^T = (E(R)\mathbf{z}) \cdot \mathbf{Q}. \end{aligned} \quad (47)$$

We may denote this action of T_d on \mathbb{R}^8 or Ω_3 in the following compact form:

$$R \rightarrow \text{Ad}(R) = T_1(R) \oplus T_2(R) \oplus E(R), \quad (48)$$

where the matrices $T_1(R)$, $T_2(R)$, $E(R)$ are defined through Eq. (47).

We list below the matrices $T_1(R)$, $T_2(R)$, $E(R)$ corresponding to $\text{Ad}(R)$ for each $R \in T_d$, and these are to be read as

$$R \in T_d \subset SU(3) \rightarrow T_1(R) \oplus T_2(R) \oplus E(R) = \text{Ad}(R)$$

$$\begin{pmatrix} 1 & 0 & 0 \\ 0 & 1 & 0 \\ 0 & 0 & 1 \end{pmatrix} \rightarrow \begin{pmatrix} 1 & 0 & 0 \\ 0 & 1 & 0 \\ 0 & 0 & 1 \end{pmatrix} \oplus \begin{pmatrix} 1 & 0 & 0 \\ 0 & 1 & 0 \\ 0 & 0 & 1 \end{pmatrix} \oplus \begin{pmatrix} 1 & 0 \\ 0 & 1 \end{pmatrix}$$

$$\begin{pmatrix} 1 & 0 & 0 \\ 0 & -1 & 0 \\ 0 & 0 & -1 \end{pmatrix} \rightarrow \begin{pmatrix} -1 & 0 & 0 \\ 0 & -1 & 0 \\ 0 & 0 & 1 \end{pmatrix} \oplus \begin{pmatrix} -1 & 0 & 0 \\ 0 & -1 & 0 \\ 0 & 0 & 1 \end{pmatrix} \oplus \begin{pmatrix} 1 & 0 \\ 0 & 1 \end{pmatrix}$$

$$\begin{pmatrix} 1 & 0 & 0 \\ 0 & 0 & 1 \\ 0 & -1 & 0 \end{pmatrix} \rightarrow \begin{pmatrix} 0 & 1 & 0 \\ -1 & 0 & 0 \\ 0 & 0 & 1 \end{pmatrix} \oplus \begin{pmatrix} 0 & 1 & 0 \\ -1 & 0 & 0 \\ 0 & 0 & -1 \end{pmatrix} \oplus \begin{pmatrix} \frac{1}{2} & \frac{\sqrt{3}}{2} \\ \frac{\sqrt{3}}{2} & -\frac{1}{2} \end{pmatrix}$$

$$\begin{pmatrix} 1 & 0 & 0 \\ 0 & 0 & -1 \\ 0 & 1 & 0 \end{pmatrix} \rightarrow \begin{pmatrix} 0 & -1 & 0 \\ 1 & 0 & 0 \\ 0 & 0 & 1 \end{pmatrix} \oplus \begin{pmatrix} 0 & -1 & 0 \\ 1 & 0 & 0 \\ 0 & 0 & -1 \end{pmatrix} \oplus \begin{pmatrix} \frac{1}{2} & \frac{\sqrt{3}}{2} \\ \frac{\sqrt{3}}{2} & -\frac{1}{2} \end{pmatrix}$$

$$\begin{pmatrix} 0 & -1 & 0 \\ -1 & 0 & 0 \\ 0 & 0 & -1 \end{pmatrix} \rightarrow \begin{pmatrix} -1 & 0 & 0 \\ 0 & 0 & 1 \\ 0 & 1 & 0 \end{pmatrix} \oplus \begin{pmatrix} 1 & 0 & 0 \\ 0 & 0 & 1 \\ 0 & 1 & 0 \end{pmatrix} \oplus \begin{pmatrix} -1 & 0 \\ 0 & 1 \end{pmatrix}$$

$$\begin{pmatrix} 0 & -1 & 0 \\ 1 & 0 & 0 \\ 0 & 0 & 1 \end{pmatrix} \rightarrow \begin{pmatrix} 1 & 0 & 0 \\ 0 & 0 & -1 \\ 0 & 1 & 0 \end{pmatrix} \oplus \begin{pmatrix} -1 & 0 & 0 \\ 0 & 0 & -1 \\ 0 & 1 & 0 \end{pmatrix} \oplus \begin{pmatrix} -1 & 0 \\ 0 & 1 \end{pmatrix}$$

$$\begin{pmatrix} 0 & 1 & 0 \\ 1 & 0 & 0 \\ 0 & 0 & -1 \end{pmatrix} \rightarrow \begin{pmatrix} -1 & 0 & 0 \\ 0 & 0 & -1 \\ 0 & -1 & 0 \end{pmatrix} \oplus \begin{pmatrix} 1 & 0 & 0 \\ 0 & 0 & -1 \\ 0 & -1 & 0 \end{pmatrix} \oplus \begin{pmatrix} -1 & 0 \\ 0 & 1 \end{pmatrix}$$

$$\begin{pmatrix} 0 & 1 & 0 \\ -1 & 0 & 0 \\ 0 & 0 & 1 \end{pmatrix} \rightarrow \begin{pmatrix} 1 & 0 & 0 \\ 0 & 0 & 1 \\ 0 & -1 & 0 \end{pmatrix} \oplus \begin{pmatrix} -1 & 0 & 0 \\ 0 & 0 & 1 \\ 0 & -1 & 0 \end{pmatrix} \oplus \begin{pmatrix} -1 & 0 \\ 0 & 1 \end{pmatrix}$$

$$\begin{pmatrix} 0 & 0 & -1 \\ 0 & -1 & 0 \\ -1 & 0 & 0 \end{pmatrix} \rightarrow \begin{pmatrix} 0 & 0 & -1 \\ 0 & -1 & 0 \\ -1 & 0 & 0 \end{pmatrix} \oplus \begin{pmatrix} 0 & 0 & 1 \\ 0 & 1 & 0 \\ 1 & 0 & 0 \end{pmatrix} \oplus \begin{pmatrix} \frac{1}{2} & -\frac{\sqrt{3}}{2} \\ -\frac{\sqrt{3}}{2} & -\frac{1}{2} \end{pmatrix}$$

$$\begin{pmatrix} 0 & 0 & -1 \\ 0 & 1 & 0 \\ 1 & 0 & 0 \end{pmatrix} \rightarrow \begin{pmatrix} 0 & 0 & 1 \\ 0 & 1 & 0 \\ -1 & 0 & 0 \end{pmatrix} \oplus \begin{pmatrix} 0 & 0 & -1 \\ 0 & -1 & 0 \\ 1 & 0 & 0 \end{pmatrix} \oplus \begin{pmatrix} \frac{1}{2} & -\frac{\sqrt{3}}{2} \\ -\frac{\sqrt{3}}{2} & -\frac{1}{2} \end{pmatrix}$$

$$\begin{pmatrix} 0 & 0 & 1 \\ 0 & 1 & 0 \\ -1 & 0 & 0 \end{pmatrix} \rightarrow \begin{pmatrix} 0 & 0 & -1 \\ 0 & 1 & 0 \\ 1 & 0 & 0 \end{pmatrix} \oplus \begin{pmatrix} 0 & 0 & 1 \\ 0 & -1 & 0 \\ -1 & 0 & 0 \end{pmatrix} \oplus \begin{pmatrix} \frac{1}{2} & -\frac{\sqrt{3}}{2} \\ -\frac{\sqrt{3}}{2} & -\frac{1}{2} \end{pmatrix}$$

$$\begin{pmatrix} 0 & 0 & 1 \\ 0 & -1 & 0 \\ 1 & 0 & 0 \end{pmatrix} \rightarrow \begin{pmatrix} 0 & 0 & 1 \\ 0 & -1 & 0 \\ 1 & 0 & 0 \end{pmatrix} \oplus \begin{pmatrix} 0 & 0 & -1 \\ 0 & 1 & 0 \\ -1 & 0 & 0 \end{pmatrix} \oplus \begin{pmatrix} \frac{1}{2} & -\frac{\sqrt{3}}{2} \\ -\frac{\sqrt{3}}{2} & -\frac{1}{2} \end{pmatrix}$$

Computing the characters (traces) of the matrices $T_1(R)$ and comparing with the character table of T_d , we see that $T_1(R)$ is actually nothing but the irreducible representation T_1 of T_d . Similarly, $T_2(R)$ and $E(R)$ are verified to be the irreducible representations T_2 and E respectively. It is in anticipation of this result that the matrices $T_1(R)$, $T_2(R)$, $E(R)$ were so named in the defining equations (47). We have thus verified that the adjoint

representation of $T_d \in SU(3)$, the symmetry group of our obese-tetrahedron, is simply the direct sum of three standard inequivalent irreducible representations of T_d .

We conclude this discussion of the symmetry of the obese-tetrahedron with several comments. Firstly, we know that $\text{Ad}(R)$, the image of $R \in T_d \subset SO(3) \subset SU(3)$ in the adjoint representation, is an element of $SO(8)$, and hence should have positive determi-

nant. This, however, does not necessarily require that $T_1(R)$, $T_2(R)$, and $E(R)$ should individually have positive determinant. In particular, two of them can have negative determinants. We note that $T_2(R)$ has positive determinant for all ‘proper’ rotations in T_d , but negative determinant for all the ‘improper’ ones, namely the S_4 ’s and σ_d ’s, the signature in the latter case being compensated by the signature of the determinant of $E(R)$. Since T_2 is a vector representation, the above remark shows that the triplet $X = (\lambda_1, \lambda_4, \lambda_6)$ transforms as a vector. On the other hand $T_1(R)$ has positive determinant for all $R \in T_d$, including the improper ones. That is, $T_1(R)$ supported by the triplet \mathbf{Y} is a pseudo-vector representation. This is consistent with the fact that this triplet actually comprises components of a pseudo-vector, the angular momentum.

Secondly, it may be noted that R and $T_1(R)$ have the same character for every $R \in T_d$. Thus it should be expected that the two representations, R and $T_1(R)$, are necessarily related by a change of basis. The required change of basis is not hard to trace. Recall that we listed the components of J as $(\lambda_2, \lambda_5, \lambda_7)$, whereas the more appropriate listing for components of angular momentum [generators of $SO(3)$] is $(\lambda_7, -\lambda_5, \lambda_2)$. Thus the change of basis which will repair the listing is effected by

$$R_0 = \begin{pmatrix} 0 & 0 & 1 \\ 0 & -1 & 0 \\ 1 & 0 & 0 \end{pmatrix} \in SO(3) \subset SU(3). \quad (49)$$

It can readily be verified that

$$R_0 T_1(R) R_0^T = R, \quad \forall R \in T_d \subset SO(3) \subset SU(3). \quad (50)$$

Finally, the above analysis has at play in an interesting manner the relationship among the full octahedral group O_h of order 48, the subgroup O comprising the proper rotations, and the tetrahedral subgroup T_d . The center of O_h is $Z_2 = (E, i)$ consisting of the identity and inversion, and we have this important connection $O \times Z_2 = O_h = T_d \times Z_2$. The centre (of any group) acts trivially in the adjoint representation, and it is for this reason that the full set of 48 generalized permutation matrices acts in the adjoint representation ‘as O ’ on the linear span of $\lambda_2, \lambda_5, \lambda_7$ while it acts ‘as T_d ’ on the linear span of $\lambda_1, \lambda_4, \lambda_6$.

VII. FINAL REMARKS

We have presented in this paper a detailed analysis of the structure of the generalized Bloch sphere Ω_3 , the state space of the qutrit. We based our analysis on closed-form expressions for Ω_3 and its boundary $\partial\Omega_3$. That these expressions are nearly as economical in form as the

case of qubit was noted. Three special concentric spheres of radii 1, $1/\sqrt{3}$, and $1/2$ in \mathbb{R}^8 were noted along with their relevance to the structure of Ω_3 .

We classified the 28 standard two-sections of Ω_3 into five unitary equivalence classes of only four different geometrically inequivalent shapes. That there are two different sets of circular two-sections that are unitarily inequivalent but geometrically equivalent was noted, a feature missed by earlier authors. The 56 standard three-sections were classified into ten unitary equivalence classes of only seven different geometrically inequivalent shapes, correcting and completing an earlier classification by Mendes [8]. The obese-tetrahedral three-section was examined in considerable detail, clarifying how its tetrahedral symmetry consisting of both proper and improper rotations arises from the $SO(3) \subset SU(3)$ group of proper rotations.

Finally, our derivation of closed-form expressions for Ω_3 and its boundary $\partial\Omega_3$ was based on the elementary observation that a singular matrix of the form $\mathbb{I} + \sqrt{3}\mathbf{n} \cdot \boldsymbol{\lambda}$, $\mathbf{n} \in \mathbb{R}^8$ cannot be indefinite if $\mathbf{n} \cdot \mathbf{n} \leq 1$. We could have used instead the following general procedure [38, 39]. Suppose we wish to characterize positivity of the $d \times d$ matrix $\mathbb{I} + H$ where H is hermitian. We may begin by evaluating $\det(y\mathbb{I} + H)$ where y is a real variable. The result will clearly be a polynomial in y of degree d :

$$\begin{aligned} P(y) &\equiv \det(y\mathbb{I} + H) \\ &= y^d + c_1 y^{d-1} + c_2 y^{d-2} + \dots + c_{d-1} y + c_d. \end{aligned}$$

All the coefficients c_j are determined by the (unitarily invariant) traces $\text{tr } H, \text{tr } H^2, \dots, \text{tr } H^d$ of H . In particular, $c_1 = \text{tr } H$ and $c_d = \det H$. [$\det H$ too is determined by the above invariant traces.]

It is now clear that a necessary and sufficient set of conditions for positivity of $\mathbb{I} + H$ is

$$P(y) \Big|_{y=1} \geq 0, \quad \frac{dP(y)}{dy} \Big|_{y=1} \geq 0, \quad \dots, \quad \frac{d^{d-1}P(y)}{dy^{d-1}} \Big|_{y=1} \geq 0.$$

This characterization of positivity was used in [38, 39] to characterize variance matrix of a multimode quantum system in a covariant manner. More recently, similar procedure has been used to characterize Ω_d [11]. Since we are dealing with the particular case $d = 3$, rather than arbitrary d , we have preferred to base our characterization of Ω_3 on the elementary observation mentioned above, rather than on this general procedure.

Acknowledgement: The authors are grateful to Prof. Rajiah Simon for permitting them to make liberal use, in Section 6, of his unpublished Lecture Notes on *Point Groups*.

[1] F.J. Bloore, Jour. Phys. A: Math. Gen. **9**, 2059 (1976).

[2] G. Ramachandran and M.V.N. Murthy, Nucl. Phys. A

- 323**, 403-412 (1979).
- [3] G. Ramachandran and M.V.N. Murthy, Nucl. Phys. A **337**, 301-312 (1980).
- [4] F.T. Hioe and J.H. Eberly, Phys. Rev. Lett. **47**, 838-841 (1981).
- [5] J. Pöttinger and K. Lendi, Phys. Rev. A **31**, 1299-1309 (1985).
- [6] G. Kimura, Phys. Lett. A **314**, 339-349 (2003).
- [7] G. Kimura and A. Kossakowski, Open Sys. & Information Dyn. **12**, 207-229 (2005).
- [8] I.P. Mendas, Jour. Phys. A: Math. Gen. **39**, 11313 (2006).
- [9] L. Jakobczyk and M. Siennicki, Phys. Lett. A **286**, 383 (2001).
- [10] S. Kryszewski and M. Zachcial, Jour. Phys. A: Math. Gen. **39**, 5921-5931 (2006).
- [11] M.S. Byrd and N. Khaneja, Phys. Rev. A **68**, 062322 (2003).
- [12] I.P. Mendas, Jour. Math. Phys. **49**, 092102 (2008).
- [13] R.A. Bertlmann and P. Krammer, Jour. Phys. A: Math. Theor. **41**, 235303 (2008).
- [14] P. Krammer, Jour. Phys. A: Math. Theor. **42**, 065305 (2009).
- [15] R.A. Bertlmann and P. Krammer, Phys. Rev. A **77**, 024303 (2008).
- [16] R.A. Bertlmann and P. Krammer, Phys. Rev. A **78**, 014303 (2008).
- [17] R.A. Bertlmann and P. Krammer, Ann. Phys. A **324**, 1388-1407 (2009).
- [18] A. Kossakowski, Open Sys. & Information Dyn. **10**, 213-220 (2003).
- [19] G. Kimura and A. Kossakowski, Open Sys. & Information Dyn. **11**, 343-358 (2004).
- [20] M.S. Byrd, C.A. Bishop, and Y.C. Ou, Phys. Rev. A **83**, 012301 (2011).
- [21] Y.C. Ou and M.S. Byrd, Phys. Rev. A **82**, 022325 (2010).
- [22] A. Checinska and K. Wódkiewicz, Phys. Rev. A **80**, 032322 (2009).
- [23] K. Dixit and E.C.G. Sudarshan, Phys. Rev. A **78**, 032308(2008).
- [24] S. Simon, S.P. Rajagopalan, and R. Simon, Pramana— Jour. Phys. **73**, 471-483 (2009).
- [25] K. Dietz, Jour. Phys. A: Math. Gen. **39**, 1433-1447 (2006).
- [26] L.J. Boya and K. Dixit, Phys. Rev. A **78**, 042108 (2008).
- [27] S.G. Schirmer, T. Zhang, and J.V. Leahy, Jour. Phys. A: Math. Gen. **37**, 1389-1402 (2004).
- [28] P.S. Bourdon and H.T. Williams, Phys. Rev. A **69**, 022314 (2004).
- [29] D.M. Appleby, A. Ericsson, and C.A. Fuchs, Found. Phys. **41**, 564-579 (2011).
- [30] S. Vinjanampathy and A.R.P. Rau, Jour. of Phys. A: Math. Theor. **42**, 425303 (2009).
- [31] T. Tilma, M. Byrd and E.C.G. Sudarshan, Jour. of Phys. A: Math. Gen. **35**, 10445 (2002).
- [32] R. Mosseri and R. Dandoloff, Jour. of Phys. A: Math. Gen. **34**, 10243 (2001).
- [33] B.A. Tay and H. Zainuddin, Chin. Phys. Lett. **25**, 6, 1923 (2008).
- [34] G. Khanna, S. Mukhopadhyay, R. Simon and N. Mukunda, Ann. Phys. **253**, 55-82 (1997).
- [35] K.S. Mallesh and N. Mukunda, Pramana — Jour. Phys. **49**, 371 (1997).
- [36] Arvind, K.S. Mallesh and N. Mukunda, Jour. Phys. A: Math. Gen. **30**, 2417 (1997).
- [37] E. Ercolessi, G. Marmo, G. Morandi, and N. Mukunda, Int. Jour. Mod. Phys. A **16**, 5007-5032 (2001).
- [38] R. Simon, E.C.G. Sudarshan, and N. Mukunda, Phys. Rev. A **36**, 3868-3880 (1987).
- [39] R. Simon, E.C.G. Sudarshan, and N. Mukunda, Phys. Lett. A **124**, 223-228 (1987).